





# Dependence on clade II bHLH transcription factors for nursing of haploid products by tapetal-like cells is conserved between moss sporangia and angiosperm anthers

Mauricio Lopez-Obando<sup>1,2\*</sup> , Katarina Landberg<sup>1\*</sup> , Eva Sundberg<sup>1</sup>  and Mattias Thelander<sup>1</sup> 

<sup>1</sup>Department of Plant Biology, The Linnean Centre of Plant Biology in Uppsala, Swedish University of Agricultural Sciences, PO Box 7080, Uppsala SE-75007, Sweden; <sup>2</sup>VEDAS Corporación de Investigación e Innovación (VEDASCII), Cl 8 B 65-261 050024, Medellín, Colombia

## Summary

Authors for correspondence:

Mattias Thelander

Email: Mattias.Thelander@slu.se

Mauricio Lopez-Obando

Email: Mauricio.obando@vedascii.org

Received: 23 September 2021

Accepted: 28 December 2021

New Phytologist (2022) 235: 718–731

doi: 10.1111/nph.17972

**Key words:** basic helix–loop–helix, bryophytes, moss, *Physcomitrium patens*, sporangium, sporogenesis, tapetum, transcription factor.

- Clade II basic helix–loop–helix transcription factors (bHLH TFs) are essential for pollen production and tapetal nursing functions in angiosperm anthers. As pollen has been suggested to be related to bryophyte spores by descent, we characterized two *Physcomitrium* (*Physcomitrella*) *patens* clade II bHLH TFs (*PpbHLH092* and *PpbHLH098*), to test if regulation of sporogenous cells and the nursing cells surrounding them is conserved between angiosperm anthers and bryophyte sporangia.
- We made CRISPR–Cas9 reporter and loss-of-function lines to address the function of *PpbHLH092/098*. We sectioned and analyzed WT and mutant sporophytes for a comprehensive stage-by-stage comparison of sporangium development.
- Spore precursors in the *P. patens* sporangium are surrounded by nursing cells showing striking similarities to tapetal cells in angiosperms. Moss clade II bHLH TFs are essential for the differentiation of these tapetal-like cells and for the production of functional spores.
- Clade II bHLH TFs provide a conserved role in controlling the sporophytic somatic cells surrounding and nursing the sporogenous cells in both moss sporangia and angiosperm anthers. This supports the hypothesis that such nursing functions in mosses and angiosperms, lineages separated by c. 450 million years, are related by descent.

## Introduction

The monophyletic group of land plants differ from the aquatic streptophytic algae from which they evolved by having both haploid and diploid multicellular generations (Graham *et al.*, 2000; Renzaglia *et al.*, 2000; Ligrone *et al.*, 2012; Harrison *et al.*, 2017). A dominant haploid generation with a subordinate diploid sporophyte specialized in the production and dispersal of spores is a trait likely to have been inherited from ancestral land plants to bryophytes, possibly representing the most basal group of extant land plants. Accordingly, the three bryophyte lineages of mosses, hornworts and liverworts all develop nonbranched sporophytes consisting of a foot and an apical capsule (sporangium) in which sporogenous cells undergo meiosis to form spores with a resistant spore wall.

Angiosperms differ from bryophytes by having a dominant diploid sporophyte generation combined with extremely reduced haploid generations (Graham *et al.*, 2000; Renzaglia *et al.*, 2000; Ligrone *et al.*, 2012; Harrison *et al.*, 2017). Fertilization depends

on male gamete delivery mediated by pollen produced in diploid anthers (Goldberg *et al.*, 1993; Gomez *et al.*, 2015; Åstrand *et al.*, 2021). In the model plant *Arabidopsis*, the anther develops microsporocytes in locules surrounded by distinct somatic cell layers, the innermost being the tapetum (Sanders *et al.*, 1999). The microsporocytes undergo meiosis to form haploid microspores, which develop into pollen through specialized mitotic divisions resulting in two male gametes contained within the cytoplasm of a vegetative cell (Berger & Twell, 2011). Meanwhile, a resistant multilayered wall, partly consisting of the complex biopolymer sporopollenin, is formed around the developing pollen (Ma *et al.*, 2021). The formation and maturation of pollen is strictly dependent on nutrients, enzymes, signals and wall components provided by the diploid somatic tapetum layer (Goldberg *et al.*, 1993; Lei & Liu, 2020). In fact, the diploid tapetum layer is sacrificed for the benefit of the newly established haploid generation as it undergoes programmed cell death to complete its nursing functions (Parish & Li, 2010).

By contrast, bryophyte male gametes consist of motile flagellated sperm produced by male reproductive organs formed in the haploid gametophyte generation (Renzaglia *et al.*, 2000; Hackenberg &

\*These authors contributed equally to this work.

Twell, 2019). Male gametogenesis in bryophytes is believed to reflect that of ancestral land plants while the pollen-based gametogenesis of angiosperms is a derived state (Hackenberg & Twell, 2019). It is not trivial to picture how pollen evolved from an ancestral state reminiscent of that in extant bryophytes, but the prevailing hypothesis is that angiosperm pollen evolved from bryophyte-like spores (Hackenberg & Twell, 2019, and references therein).

The homology between bryophyte spores and angiosperm pollen is supported by the inclusion of the biopolymer sporopollenin in the outer walls of both. Homologs to angiosperm genes encoding enzymes essential for proper sporopollenin pollen wall formation (*PpASCL*, *PpMS2* and *PpCYP703B1/2*) and transcription factors (TFs) regulating the expression of those genes (*PpGAMYB1/2*) are all needed for proper spore wall formation in the bryophyte model moss *Physcomitrium patens* (Aya *et al.*, 2011; Colpitts *et al.*, 2011; Wallace *et al.*, 2015; Daku *et al.*, 2016). Some of these moss genes are expressed in both the sporogenous cells and the cells immediately surrounding them, and manipulation of their expression can affect the deposition/distribution of sporopollenin matter in the spore chamber (Aya *et al.*, 2011; Wallace *et al.*, 2015; Daku *et al.*, 2016). While this indicates that the cells surrounding the sporogenous cells in moss are likely to provide the developing spores with wall material, much like anther tapetal cells, the extent of common regulation and function of these possibly distantly related cells is still unclear.

In angiosperms, the specification and function of tapetal cells is tightly controlled by a cascade of TFs (Gomez *et al.*, 2015; Verma *et al.*, 2019). At the heart of this regulation lies basic helix–loop–helix (bHLH) TFs belonging to the land plant-specific clades II and III(a+c)1 (Catarino *et al.*, 2016; Zheng *et al.*, 2020). Loss of function in any of these two bHLH subfamilies is detrimental to tapetal functions, and hence to the production of functional pollen, both in monocots such as rice and in dicots such as *Arabidopsis* (Sorensen *et al.*, 2003; Jung *et al.*, 2005; Li *et al.*, 2006; Zhang *et al.*, 2006; Xu *et al.*, 2010; Niu *et al.*, 2013; Fu *et al.*, 2014; Ko *et al.*, 2014; Zhu *et al.*, 2015). Homologs belonging to these two bHLH subfamilies are clearly identifiable also in bryophytes (Pires & Dolan, 2010; Catarino *et al.*, 2016; Zhang *et al.*, 2020), and it was recently hypothesized that tapetal-like tissues and their control by bHLH TFs could have been established already in the common ancestors of bryophytes and angiosperms (Zheng *et al.*, 2020).

We here report the functional characterization of two closely related clade II bHLH TFs, *PpbHLH092* and *PpbHLH098*, in the bryophyte model moss *P. patens*. We show that the genes exert their functions in the moss sporangium where they are redundantly needed for the production of spores and for the nursing of sporogenous cells by surrounding somatic cells. This shows that clade II bHLH TFs are functionally conserved between mosses and angiosperms and supports the hypothesis that cells nursing developing spores in mosses and pollen in angiosperms are related by descent.

## Materials and Methods

### Plant material, growth conditions and tissue harvest

The *P. patens* ecotype Reute (Hiss *et al.*, 2017) was used as the wild-type (WT) and background for transgenic lines. For subcultivation, moss was grown in constant white light at  $30 \mu\text{mol m}^{-2} \text{s}^{-1}$  using side irradiation in a Sanyo MLR-350 chamber at 25°C. For phenotypic analysis, protonema was subcultivated twice for 7 d on cellophane-covered BCD media (Thelander *et al.*, 2007) supplemented with 5 mM ammonium tartrate and 0.8% agar. Protonemal tissue, shaped into 1–2 mm balls, was then placed on solid BCD medium supplemented with 0.8% agar in deep Petri dishes (90 × 25 mm; WVR PHOE305; Radnor, PA, USA) and grown for 5–6 wk. To induce reproductive organ formation and sporophyte development, the plants were transferred to short day conditions (8 h : 16 h, light : dark photoperiod) with  $30 \mu\text{mol m}^{-2} \text{s}^{-1}$  light intensity in a Sanyo MLR-350 chamber at 15°C. At  $20 \pm 1$  d of short-day incubation, plants were submerged in water overnight to increase fertilization. To prepare sporophytes for downstream analysis, gametophores (gametophyte shoots) growing in the periphery of colonies were harvested at specified time points after watering. Gametophore apices were stripped free from leaves, antheridia and nonfertilized archegonia using tweezers, leaving samples consisting of a short apical stem section terminating in a single archegonium harboring an embryo/sporophyte. From stage 8, the calyptra was excluded from samples.

### Generation of CRISPR loss-of-function mutants

Constructs expressing genomic RNAs (gRNAs) targeting exon 3 of *PpbHLH092* and *PpbHLH098* were designed using CRISPOR (Haeussler *et al.*, 2016). To produce the plasmids pMLO6-8 (Supporting Information Fig. S1a; Table S1), AttB1-PpU6-SgRNAs-AttB2 fragments produced by gene synthesis (Integrated DNA Technologies, Coralville, IA, USA) were cloned into the vector pDONR221 by Gateway recombination (Invitrogen). Inserts were confirmed by sequencing. CRISPR single and double loss-of-function mutants were then obtained as previously described (Lopez-Obando *et al.*, 2016). In short, PEG-mediated transformation (Schaefer *et al.*, 1991) was used to cotransform 8  $\mu\text{g}$  of pACT1:hCAS9, 4  $\mu\text{g}$  of pBNRF, and 4  $\mu\text{g}$  of one or two of the plasmids pMLO6-8 into WT protoplasts (pMLO6 for *PpbHLH092*, pMLO7 for *PpbHLH098*, and pMLO6 and pMLO8 for combined *PpbHLH092* and *PpbHLH098* editing). Transformants were selected on  $50 \mu\text{g ml}^{-1}$  G418 (Thermo Fisher Scientific, Waltham, MA, USA) and mutations were evaluated by PCR amplification and sequencing of gDNA with gene-specific primers. For *PpbHLH092*, primers SS647/SS648 and for *PpbHLH098* primers SS649/SS650 were used (Fig. S1a; Table S2). For phenotypic analysis, two independent lines with loss-of-function mutations were selected for each genotype (*Ppbhlh092-1/2*, *Ppbhlh098-1/2*, *Ppbhlh092Ppbhlh098-1/2*). For a summary of CRISPR-induced mutations in these lines, see Table S3.

## Generation of *PpbHLH092* translational knock-in reporter lines

Primer sequences are shown in Table S2. Inserts and fusion points of new constructs were verified by sequencing. The translational reporter construct pMLO9 (Fig. S1b), serving to integrate a GFP-GUS (green fluorescent protein and beta-glucuronidase) gene in frame near the end of the *PpbHLH092* coding sequence, was generated by the fusion of four PCR fragments using In-Fusion technology (TaKaRa Bio): a 4548 bp vector fragment amplified with primers SS657/SS658 from plasmid pDEST14 (Thermo Fisher Scientific); a fragment covering 739 bp from intron 4 to near the end of the *PpbHLH092* coding sequence (CDS) amplified with primers SS651/SS652 from WT gDNA; a fragment covering a 2556 bp GFP-GUS gene amplified with primers SS655/SS656 from plasmid pMT211 (Thelander *et al.*, 2019); and a fragment covering 502 bp of the extreme end of the CDS and the 3' untranslated region (UTR) of *PpbHLH092* amplified with primers SS653/654 from WT gDNA. To promote CRISPR-CAS9-mediated integration of the reporter in pMLO9, plasmid pMLO10 expressing a gRNA targeting the C-terminal region of *PpbHLH092* (Fig. S1b; Table S1) was generated. The annealing product of the complementary primers SS667/SS668 was cloned into the vector pENTR\_PpU6\_L1L2 opened with *BsaI* (Mallett *et al.*, 2019). Finally, to generate the *PpbHLH092pro::PpbHLH092-GFPGUS* reporter lines, 8 µg of pMLO9 and 4 µg of pMLO10 were cotransformed into WT protoplasts (Schaefer *et al.*, 1991) together with 8 µg pACT1:hCAS9 and 4 µg pBNRF (Lopez-Obando *et al.*, 2016). Stable transformants were selected on 50 µg ml<sup>-1</sup> G418 (Thermo Fisher Scientific) and integration of the pMLO9 reporter construct was evaluated by PCR confirmation of 5' and 3' junctions using the primers SS719/SS721 and SS716/SS718, respectively (Fig. S1c,d), and by PCR amplification and sequencing of the in-frame fusion between the *PpbHLH092* CDS and the GFP-GUS gene using the primers SS669/SS627 (Fig. S1b). Three independent lines showing the desired in-frame integration of the GFP-GUS gene (Table S3) were selected for histochemical GUS staining and were found to show similar expression patterns.

## GUS staining

Gametophores harboring sporophytes at different stages of development were harvested from reporter lines and settled in GUS solution (50 mM NaPO<sub>4</sub>, pH 7.2, 2 mM Fe<sup>2+</sup>CN, 2 mM Fe<sup>3+</sup>CN, 2 mM X-Gluc and 0.2% (v/v) Triton X-100). Vacuum was applied twice for 2 min and samples were incubated overnight at 37°C. Samples were then cleared in 75% ethanol.

## Sporophyte sectioning

In total, 275 WT and 187 *Ppbhlh092Ppbhlh098-1* sporophytes of different developmental stages were harvested from 1 (WT)/6 (mutant) to 37 days post-watering (dpw). Sporangia harvested after 12 dpw were impermeable, and such sporangia were

carefully perforated using a fine needle before fixation/infiltration/embedding (for 14–20 dpw sporangia this resulted in partial loss of sporogenous cells). Samples were fixed in FGPM (3% (v/v) formaldehyde, 1.5% (v/v) glutaraldehyde, 0.01% Triton X-100 in 0.1 M pH 7 Pi-buffer) overnight at 4°C, dehydrated by incubation for 20 min each in 10, 30, 50, 70, 85, 95 and 99.5% ethanol, preinfiltrated in a 1 : 1 solution of 99.5% ethanol : infiltration solution (50 ml historesin base and 0.5 g activator powder from Leica historesin embedding kit #7022 31731 supplemented with 1 ml PEG400) for 3 h at room temperature, and finally infiltrated overnight in concentrated infiltration solution. Embedding in a 15 : 1 mix of infiltration solution and hardener was carried out at room temperature in plastic Histomolds of 6 × 8 mm (Leica). Longitudinal sections 6 µm thick obtained using a Microm HM 355S microtome with a glass knife were transferred to water-covered microscopy slides kept on a 42°C heating table. Once the water had evaporated, the dried-in sections were stained in 0.01% Toluidine blue (w/v, 0.1 M phosphate buffer pH 7.0) for 2 min and washed three times in water for 1 min. Sections of GUS-stained *PpbHLH092pro::PpbHLH092-GFPGUS* sporophytes were produced in the same way, but here sections were made 10 µm thick and Toluidine blue staining was omitted.

## Microscopy, image processing and analysis

Images of intact nonfixed sporophytes were obtained using a MZ16 stereo microscope, a DFC295 camera and LAS AF software (Leica Microsystems, Wetzlar, Germany). Images of sporogenous cells released from disrupted sporangia and mounted in 30% glycerol were obtained using a DMI4000B microscope with differential interference contrast optics, a DFC360FX camera and LAS AF software (Leica Microsystems). Images of GUS-stained sporophytes mounted in 30% glycerol and Toluidine blue- or GUS-stained sporophyte sections were obtained using an Axioscope A1 microscope, an AxioCam ICc 5 camera and Zen Blue software (Zeiss). Adobe PHOTOSHOP CC was used to adjust intensity and contrast, remove background and trace structures in figures. Numerical distance data were generated by measurements in micrographs using the IMAGEJ Fiji platform (Schindelin *et al.*, 2012). Microsoft EXCEL was used to create bar charts, calculate means and SD, and to perform Student's *t*-tests.

## RT-qPCR

Tissue samples from vegetative gametophore apices, antheridia and archegonia have been previously described (Landberg *et al.*, 2020). For the sporophyte samples, colonies with numerous adult gametophores were flooded 20 d after transfer to inductive conditions, after which 100 sporophytes of the proper developmental stage were harvested after 4 d (S1), 7–8 d (S2), 14–15 d (S3) or 37 d (S4), respectively (stages S1–4 as in Ortíz-Ramírez *et al.*, 2016). For S1 and S2 samples both the embryo/sporophyte and the surrounding archegonial mother tissues was harvested. Tissue harvest, RNA extraction, cDNA synthesis and

amplification, setup and cycling of quantitative PCRs (qPCRs), normalization using three reference genes and calculations have been previously described (Landberg *et al.*, 2020). The gene-specific primers used were SS588/SS589 for *PpbHLH092*, SS590/SS591 for *PpbHLH098*, SS712/SS713 for *PpbHLH003* and SS710/SS711 for *PpbHLH044* (Table S2). To avoid amplification of genomic DNA contamination, the annealing site for one primer in each pair is interrupted by an intron. Melt curve, gel and standard curve analyses confirmed that both primer pairs amplified a single product of the expected size with efficiencies close to 100% (data not shown). Data are presented as relative expression calculated with the  $2^{-\Delta\Delta CT}$  method, using the gene with the highest transcript abundance across the samples as the calibrator. Each data point is based on biological triplicates and error bars represent standard deviations.

### Clade II bHLH protein sequence retrieval and phylogenetic analysis

Sequences of clade II bHLH gene products from *Arabidopsis thaliana* (AtbHLH010/AT2G31220.1; AtbHLH089/AT1G06170.1; AtbHLH091/AT2G31210.1), *Medicago truncatula* (MtEAN1/Medtr4g094762.1; MtEAN2/Medtr4g094758.1), *Oryza sativa* (OsbHLH141/LOC\_Os04g51070.1; OsbHLH142/LOC\_Os01g18870.1), *Zea mays* (ZmbHLH122/AC233960.1\_FGT005; ZmbHLH16/GRMZM2G021276\_T04), *Selaginella moellendorffii* (SmbHLH037/81013; SmbHLH084/402928), *Marchantia polymorpha* (MpbHLH008/Mp2g06450.1; MpbHLH036/Mp2g04180.1; MpbHLH037/Mp2g04200.1; MpbHLH050/Mp2g04190.1) and *P. patens* (PpbHLH092/Pp3c5\_20560V3.1; PpbHLH09/Pp3c6\_8660V3.1) were obtained by BLASTP searches from Phytozome V12.1 while gene products from the fern *Salvinia cucullata* (*ScbHLH\_CII/Sacu\_v1.1\_s0019.g007717*) and the hornwort *Anthoceros agrestis OXF* (AgbHLH\_CII/AagrOXF\_evm.model.utg0000081.115.1) were obtained from [www.fernbase.org](http://www.fernbase.org) and [www.hornworts.uzh.ch](http://www.hornworts.uzh.ch), respectively. Amino acid sequences were aligned using the M-Coffee algorithm in T-COFFEE (Notredame *et al.*, 2000; Wallace *et al.*, 2006) after which they were filtered using transitive consistency scores (Chang *et al.*, 2014). The resulting filtered alignment (Fig. S2) was used for phylogenetic reconstruction in MEGAX (v.10.1.5; Kumar *et al.*, 2018) with the maximum-likelihood method (LG amino acid substitution model, gamma distribution among sites) and 500 replications of bootstrapping.

## Results

### Homologs of bHLH TFs regulating tapetum development in angiosperms are expressed in the developing *P. patens* sporophyte

The bHLH TF clades II and III(a+c)1 comprise angiosperm genes essential for tapetum and pollen development (Zheng *et al.*, 2020). Genes belonging to the same two bHLH TF clades appear to exist in all land plants (Catarino *et al.*, 2016), and in *P. patens* the clade II genes *PpbHLH092* and *PpbHLH098*, and the clade

III(a+c)1 genes *PpbHLH003* and *PpbHLH044*, are found (Zheng *et al.*, 2020). To get a first indication of where and when these moss genes are expressed, we surveyed publicly available tissue-specific gene expression data (Ortiz-Ramirez *et al.*, 2016; Perroud *et al.*, 2018; Fernandez-Pozo *et al.*, 2020). This revealed that all four genes are expressed primarily in the developing moss sporophyte (Fig. S3). To verify this, we analyzed tissue-specific transcript abundance by qPCR, which confirmed that all four genes are expressed primarily in globular sporophytes, with clade II genes showing a somewhat earlier peak than clade III(a+c)1 genes (Fig. 1a,b). To investigate if this sporophyte expression may reflect that bHLH TFs are needed for the nursing of haploid products by tapetal-like cells also in moss, we initiated a functional characterization of the clade II genes *PpbHLH092* and *PpbHLH098*.

### The clade II bHLH TFs *PpbHLH092* and *PpbHLH098* encode highly similar proteins sharing domain architecture with angiosperm homologs

*PpbHLH092* and *PpbHLH098* share the same exon–intron organization and encode proteins of 601 and 594 amino acids, respectively (Fig. 1c). A survey of *PpbHLH092* and *PpbHLH098* homologs followed by a phylogenetic analysis confirmed the existence of bHLH TFs belonging to clade II in all major land plant lineages, including ferns, lycophytes, mosses, hornworts and liverworts (Fig. 1d).

*PpbHLH092* and *PpbHLH098* are highly similar to each other throughout the lengths of their amino acid sequences (Fig. S4). By contrast, sequence conservation between the two moss proteins and their *Arabidopsis* and rice homologs is largely limited to the central bHLH domain and a C-terminal BIF domain, demonstrated in angiosperms to mediate regulatory interactions with other bHLH TFs (Figs 1e,f, S4; Cui *et al.*, 2016; Zheng *et al.*, 2020). Striking sequence similarity is largely restricted to the same two domains also when functionally conserved homologs from dicots and monocots are compared (Fig. S4), suggesting that clade II bHLH TFs could potentially be functionally conserved also between bryophytes and angiosperms.

### The two clade II bHLH TFs are together essential for spore production

To elucidate the function of *PpbHLH092* and *PpbHLH098*, we generated single and double loss-of-function mutants by CRISPR-Cas9 using single guide RNAs (sgRNAs) targeting regions of exon 3 located upstream of the sequences encoding the conserved bHLH and BIF domains (Fig. S1a; Table S1). For each sgRNA used, putative off-targets had at least four mismatches making off-target editing events highly unlikely (Table S1; Modrzejewski *et al.*, 2020). Two independent lines of each genotype (*Ppbhlh092-1/2*, *Ppbhlh098-1/2*, *Ppbhlh092Ppbhlh098-1/2*) with mutations in the relevant gene (s) likely to block protein function (Table S3) were selected for phenotypic analysis.



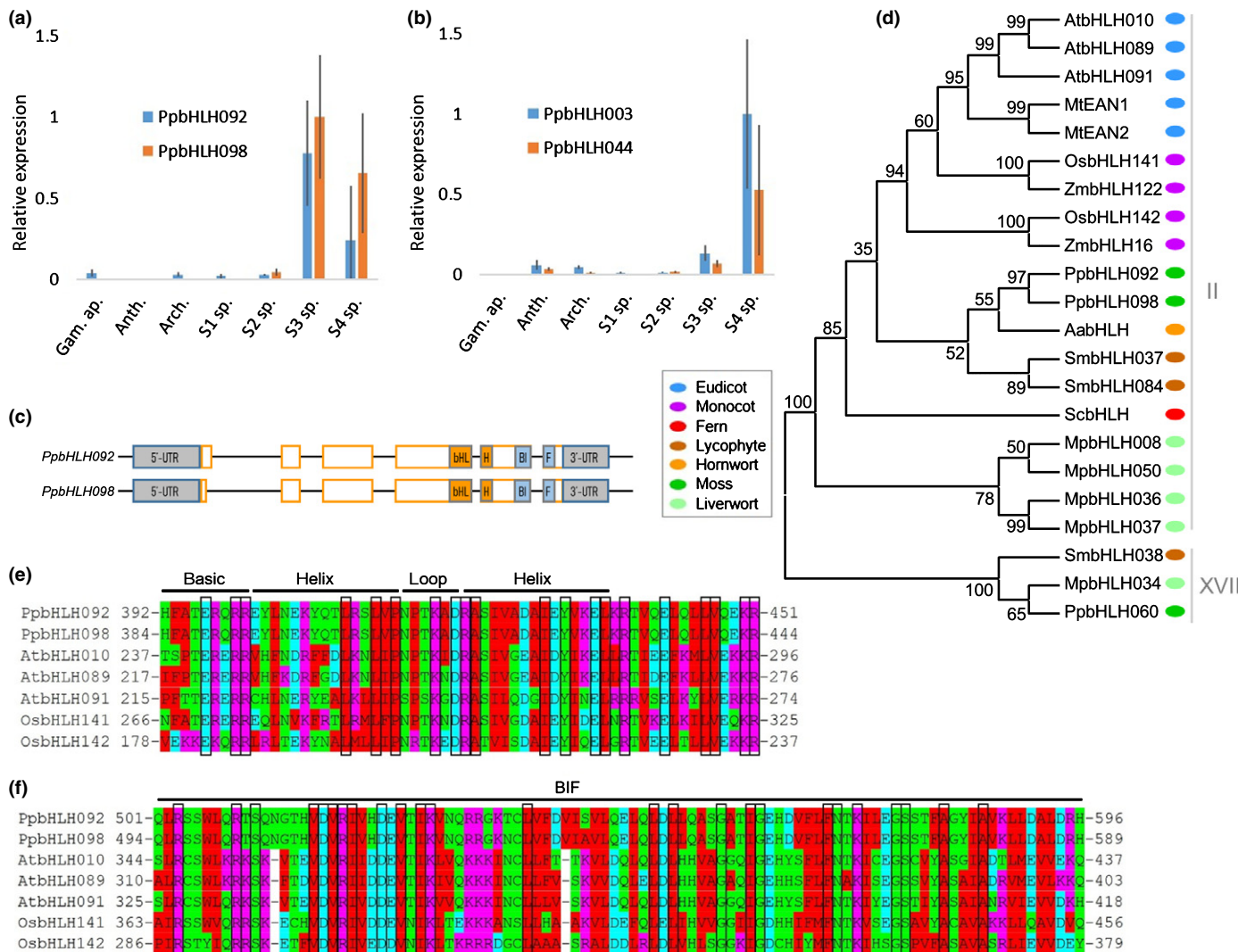


**Fig. 1** Expression, architecture and sequence conservation of the *Physcomitrium patens* proteins *PpbHLH092* and *PpbHLH098*. (a, b) Relative transcript abundance of *PpbHLH092/098* (a) and *PpbHLH003/044* (b) assayed by qPCR in gametophore apices (Gam. ap.), antheridia (Anth.), archegonia (Arch.) and sporophytes (sp.) at developmental stages as defined by Ortíz-Ramírez *et al.* (2016). Each data point represents an average of three independent biological replicates and error bars indicate standard deviation. (c) Schematic representation of *PpbHLH092* and *PpbHLH098* indicating their identical exon/intron and domain organization. Flanking untranslated regions (UTR) are colored in gray, central bHLH domains are colored in orange and C-terminal BIF domains are colored in light blue. (d) Phylogeny of clade II bHLH TFs from representative land plant species. At, *Arabidopsis thaliana* (dicot); Mt, *Medicago truncatula* (dicot); Os, *Oriza sativa* (monocot); Sc, *Salvinia cucullata* (fern); Sm, *Selaginella moellendorffii* (lycophyte); Pp, *P. patens* (moss); Aa, *Anthoceros agrestis* (Oxford; hornwort); Mp, *Marchantia polymorpha* (liverwort). Selected genes from clade XVII bHLH TFs were included as an outgroup. (e) Amino acid sequence alignment of central bHLH domains from clade II bHLH TFs in *P. patens*, *Arabidopsis* and rice. (f) Amino acid sequence alignment of the C-terminal BIF domains from clade II bHLH TFs in *P. patens* (moss), *Arabidopsis* (dicot) and rice (monocot). In (e, f), positions showing identical residues are boxed while similar amino acids are marked by the same color. For a full amino acid sequence alignment including all bHLH clade II proteins represented in (d), see Supporting Information Fig. S4.

We could not detect any obvious alterations in the growth or development of the haploid gametophyte generation in the single and double mutants. Thus, development of vegetative filamentous protonema and gametophores, as well as of male and female reproductive organs, progressed as in the WT (data not shown). Even if subtle differences do exist, the *Ppbhl092* and *Ppbhl098* single mutants lacked obvious phenotypic deviations also in the diploid sporophyte and were able to produce germination-competent spores at normal rates (data not shown). By contrast, the *Ppbhl092Ppbhl098* double mutants consistently showed

striking alterations in the sporophyte generation. Only data from one double mutant line are shown in most figures and graphs below because the two independent lines exhibited an identical phenotype.

The mature *P. patens* sporophyte consists of an apical sporangium (spore capsule) connected via a short seta to a foot anchored in gametophytic mother tissues. We achieved a synchronized onset of sporophyte development, allowing systematic comparisons of WT and *Ppbhl092Ppbhl098* double mutant sporophytes by flooding the moss gametophores to boost

fertilization when fertilization competency had just been reached. External examination revealed that WT and double mutant sporophytes appeared morphologically identical without significant differences in sporangium width up until 12 dpw, a stage when radial expansion of the green sporangium is highly active (Fig. 2a,b).

Radial expansion of the WT sporangium slows down successively between 12 and 16 dpw, and thereafter spore formation, marked by a change of sporangium color from light green to dark brown, becomes evident (Fig. 2b; Daku *et al.*, 2016; Hiss *et al.*, 2017). By contrast, expansion of *Ppbhlh092Ppbhlh098* double mutant sporangia started to lag behind from 14 dpw and they also failed to show browning (Fig. 2a,b). Instead, double mutant sporangia stayed light green at least until 37 dpw, well beyond the time point when mature spores are released from the WT. A subset of double mutant sporangia eventually showed some light internal browning, but this is attributed to tissue degeneration (see second last section of results). These observations suggest that *Ppbhlh092Ppbhlh098* double mutants are affected in spore formation and/or maturation. In line with this, double mutant sporangia failed to release spores when punctured even after months of incubation.

### Clade II bHLH TFs are dispensable for the cell division phase of sporangium patterning

To unravel the details behind the developmental arrest of double mutant sporangia, we sectioned longitudinally and analyzed 275 WT and 187 *Ppbhlh092Ppbhlh098* sporophytes ranging from early embryos to mature specimens. We expanded previous descriptions of *P. patens* sporophyte ontogeny and divided it into 15 distinct stages based on morphological characters related to sporangium patterning and maturation (Table 1; Figs 3a, S5a; Sakakibara *et al.*, 2008; Kofuji *et al.*, 2009; Daku *et al.*, 2016; Yip *et al.*, 2016; Coudert *et al.*, 2019). To gain details about the temporal and spatial distribution of clade II bHLH TFs during sporophyte

development we also produced translational knock-in reporters for *PpbHLH092* by CRISPR-CAS9-mediated insertion of a GFP-GUS gene just before its stop codon (Fig. S1b). This resulted in three independent *PpbHLH092pro::PpbHLH092-GFP-GUS* lines exhibiting informative and identical GUS staining patterns (see below) while GFP signals were below the detection level.

After fertilization, the WT *P. patens* zygote undergoes a transversal division to form a basal cell contributing to the sporophyte foot and an apical stem cell cleaving off daughters in two files to promote early growth of the spindle-shaped embryo (Fig. S5a, st1; Kofuji *et al.*, 2009; Yip *et al.*, 2016). Development of the sporangium then initiates by radial expansion promoted by periclinal divisions of the subapical daughter cells, resulting in an outer amphithecium and an inner endothecium layer (Fig. S5a, st2; Yip *et al.*, 2016). Amphithecium cells undergo additional periclinal divisions, typically resulting in three cell layers eventually forming the sporangium wall (Figs 3a, S5a, st3–4). Inner endothecium cells then go through successive periclinal divisions to produce 12 cell files in a medial longitudinal section at the start of stage 8 (Figs 3a, S5a, st5–8): a core of six files making up the central columella flanked on both sides by single files of sporogenous cells surrounded by two additional layers, together often referred to as the tapetum (or the spore sac). Even if the sporogenous and tapetal cell layers surround most of the columella, medial sections clearly show that the columella is directly connected to tissues below and above it (Figs 3a, S5a, >st8). In sections, a darkly stained boundary, or even a gap (most frequent at st9), between the amphithecium and endothecium indicates the distinct nature and possible symplastic isolation of these two cell populations (Figs 3a, S5a).

We could not detect any defects in *Ppbhlh092Ppbhlh098* double mutant sporophytes up to completion of the periclinal sporangial divisions at the transition from stage 7 to 8 (Figs 3a, S5b). Consistent with this, *PpbHLH092* reporter output indicated that the gene is silent until the very end of this developmental window. Thus, the first signs of weak endothecium-specific

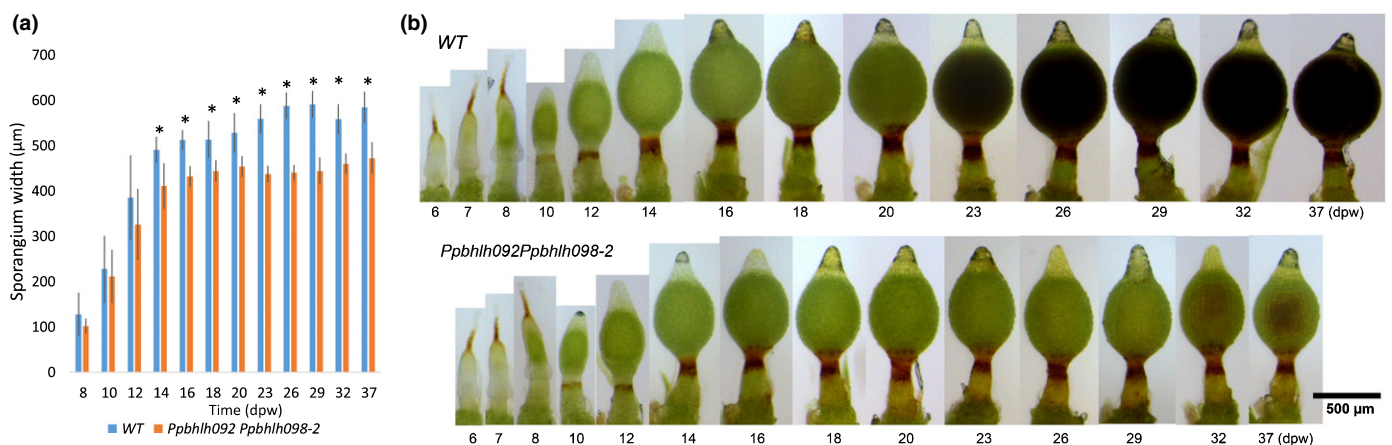


**Fig. 2** Sporangium development in the *Physcomitrium patens* *Ppbhlh092Ppbhlh098* double mutant is arrested after 12 days post-watering (dpw). (a) Bar graph showing the average width across WT and *Ppbhlh092Ppbhlh098* double mutant sporangia of different ages ( $n = 9–24$ ). Error bars indicate standard deviation and asterisks mark statistically significant differences between the two genotypes (Student's *t*-test,  $P < 0.05$ ). (b) Representative sporophytes from WT and the *Ppbhlh092Ppbhlh098-2* double mutant harvested from 6 to 37 dpw. Note that calyptra (remnants of female reproductive organ normally covering the upper part of the sporophyte) were removed from all specimen harvested after 8 dpw.

**Table 1** Wild-type (WT) sporophyte development in *Physcomitrium patens* divided into 15 stages based on sporangia characters.

Stage	Sporangium hallmarks evident in longitudinal medial sections (Fig. 3a,b, Supporting Information Fig. S5a)	Sporophyte characters evident by external examination (Fig. 2b)	dpw <sup>1</sup>	Sporophyte height (μm) <sup>2</sup>	Sporophyte width (μm) <sup>3</sup>	n <sup>4</sup>
1	1–2 cell files	The embryo is developing inside the growing translucent spheroid archegonium venter	0.9 ± 1.2	54 ± 21	36 ± 6	33
2	2 amphi- & 2 endothecium files		3.2 ± 1.1	120 ± 26	52 ± 7	21
3	4 amphi- & 2 endothecium files		4.8 ± 1.0	240 ± 50	71 ± 8	25
4	6 amphi- & 2 endothecium files	Sporophyte still developing inside the archegonium venter. Midparts of archegonial mother tissues bulge out to form a conspicuous ridge. Sporangial part of sporophyte is becoming increasingly green.	6.7 ± 0.5	383 ± 50	89 ± 5	10
5	6 amphi- & 4 endothecium files		7.1 ± 0.9	440 ± 40	101 ± 8	7
6	6 amphi- & 5–8 endothecium files		8.0 ± 0	514 ± 66	102 ± 6	6
7	6 amphi- & 9–12 endothecium files		9.0 ± 1.3	732 ± 89	152 ± 24	7
8	All primary cell layers have formed. Amphithecium cells start to expand	Archegonial mother tissue is ruptured at base of recently formed ridge. Rupture site marked by pigmented collar. Upper part of remaining mother tissues (calyptra) loose but keeps covering sporangia tip	9.8 ± 1.1	874 ± 59	214 ± 26	10
9	The single-celled sporogenous layer is distinct and stains dark blue. Columella and tapetum cells start to expand	The light green sporangium undergoes successive radial expansion until it reaches a near globular shape	11.5 ± 1.7	1131 ± 147	339 ± 71	13
10	Sporogenous cells go through final divisions and start to round up and separate. Active cytoplasm in parts of columella and tapetum cells facing sporogenous cells become evident		13.9 ± 1.7	1196 ± 90	483 ± 30	24
11	Sporogenous cells completely rounded up and clearly liberated from each other. Cell expansion of columella and tapetum completed		16.3 ± 1.5	1165 ± 76	509 ± 33	6
12	Sporogenous cells have undergone meiosis and are visible as intact held-together tetrads. Columella and tapetum undergo compaction	The near globular sporangium changes color from light green via yellow/orange to dark brown	18.2 ± 1.4	1187 ± 89	518 ± 36	21
13	Tetrads disintegrate, releasing immature spore cells.		19.2 ± 1.0	1177 ± 85	534 ± 40	25
14	Spores have started to form spore walls. Particulate matter probably deposited by columella and tapetum cells is evident in spore chamber		23.7 ± 2.4	1235 ± 70	564 ± 42	18
15	Spore wall formation is completed. Compaction of columella and tapetum layers, and also of the amphithecium/sporangium wall further pronounced	Sporangia ready to crack open so that mature spores are exposed/released	31.3 ± 4.0	1260 ± 62	579 ± 33	46

<sup>1</sup>Days post-watering when occurrence of stage peaked.

<sup>2</sup>Average length from base of foot to pointed tip of sporangium (μm, ± SD), measured in longitudinal medial sections.

<sup>3</sup>Average width across the widest part of the sporophyte (μm, ± SD), measured in longitudinal medial sections.

<sup>4</sup>Number of sectioned sporophytes analyzed.

expression are not seen until stage 7 (Fig. 4). The lack of reporter signals and mutant phenotypes in stage 1–8 sporangia shows that clade II bHLH TFs are dispensable for cell division-promoted early patterning of the moss sporangium.

When the periclinal divisions shaping the sporangium are completed at stage 8, the sporophyte foot and seta, important for the transfer of nutrients from the gametophytic tissue to the growing sporophyte, have already assumed their final organization, partly thanks to the activity of an intercalary meristem positioned proximal to the sporangium (Figs 3a, S5a; Regmi *et al.*, 2017; Coudert *et al.*, 2019). The *PpbHLH092* reporter indicated a weak expression in the foot of developing sporophytes (Fig. 4a), but we were unable to detect any developmental aberrations affecting this part of the sporophyte in the *Ppbhlh092 Ppbhlh098* double mutant (Figs 3a, S5b).

### Early functions of clade II bHLH TFs include promotion of columella expansion and termination of tapetal cell division

In WT sporangia, the columella and tapetum layers next switch to a transient expansion phase during which significant cell enlargement in three dimensions accompanied by increased vacuolarization is evident (Figs 3a, S6a,b, st9–11). During this phase, we detected *PpbHLH092* reporter signals throughout the endothecium, indicating strong expression in the columella and tapetum layers but also in the sporogenous cells (Fig. 4). Consistent with this expression, we observed a first obvious aberration in *Ppbhlh092Ppbhlh098* sporangia from around stage 9/12 dpw, manifested as reduced columella cell expansion (Figs 3a, S6b). Also, at around the same stage, we more frequently observed portions of the tapetum consisting of three cell layers, rather than



two, which is typical in the WT (Fig. 3a,b). This may indicate that termination of periclinal cell divisions in the tapetum is delayed in the double mutant. After this point, as further outlined below, WT-like sporangial development is blocked, and the stage of the double mutant sporangia from 14 dpw and onwards is referred to as 10+ in Fig. S5(b).

### Sporogenous cells arrest before meiosis in the absence of clade II bHLH TFs

While the WT columella and tapetum cells undergo expansion and vacuolarization, the sporogenous cells undergo a final set of divisions with a seemingly random division plane during stage 10 (Fig. 3a,b). These cells then retract from their original cell walls, round up and form new walls, believed to consist of mucopolysaccharides, between the plasma membranes and the original walls (Brown & Lemmon, 2013). The original cell walls soon degrade to liberate isolated globular sporocytes into the successively expanding spore chamber between the columella and the tapetum layers (Figs 3a,b, S7, st11). Thereafter, the sporocytes go through meiosis to produce tetrads consisting of four haploid spore cells enclosed by the still intact sporocyte wall (Figs 3a,b, S7, st12). The sporocyte wall is eventually ruptured to release the individual spores into the spore chamber (Figs 3a,b, S7, st13). Once freed, the spores soon acquire a conspicuous multilayered sporopollenin-containing wall (Figs 3a,b, S7, st14–15; Aya *et al.*, 2011; Colpitts *et al.*, 2011; Wallace *et al.*, 2015; Daku *et al.*, 2016).

Reporter data suggest that *PpbHLH092* expression in the sporogenous cells, as well as in the columella and tapetum, peaks at around stage 11, after which it successively declines (Fig. 4). Examination of sections of *Ppbhlb092Ppbhlb098* double mutant sporangia showed that this expression is an absolute prerequisite for the production of functional spores (Fig. 3a,b). We found that double mutant sporogenous cells did undergo the final cell divisions during stage 10 as in the WT, while further developmental progression was deficient. The double mutant sporogenous cells thus failed to round up, to completely degrade their original cell walls, to completely detach from each other, to form clearly discernible sporocyte walls, to go through meiosis or to form a discernible spore wall. Instead, the sporogenous cells of the double mutant started to shrink and were eventually degraded, which resulted in internal light browning of the sporangium.

Somatic nursing cells surrounding the sporogenous cells fail to accumulate active cytoplasm, compact/degrade and release extracellular matter in the absence of clade II bHLH TFs

By examination of WT sporophyte sections, we found that transition from premeiotic sporocytes to mature spores is accompanied by drastic and highly ordered changes affecting the columella and tapetum layers (Fig. 3b). While all columella and tapetum cells are largely vacuolated at the end of the cell expansion phase, cells in both layers positioned immediately adjacent to the

sporogenous layer stand out by possessing residual and/or reaccumulated active cytoplasm in domains directly facing the sporogenous cells during stages 10–13 (Fig. 3b). At stage 11, when liberated sporocytes have formed, expansion of the width of columella and tapetum is abruptly turned into successive width reduction, contributing to expansion of the intervening chamber in which spores mature (Figs 3a,b, S6a,b). While this reduction in layer width is due partly to compaction of cells, our observations suggest that it also may involve loss of cells immediately adjacent to the sporogenous layer. Thus, the average number of clearly discernible cells across the width of the columella is successively reduced through stages 11 to 15 in the WT (Figs 3a, S6c). Similarly, cells of the innermost tapetum layer are often not possible to spot in sections when stages 14 and 15 are reached (Fig. 3a,b). Our data do not allow us to tell with certainty whether these observations are caused by programmed cell death/degradation or compaction making cells impossible to see in sections.

The compaction and possible loss of WT columella and tapetum cells facing the spore chamber coincides with the deposition of extracellular particulate matter outside these layers at stages 14 and 15 (Fig. 3b). It appears likely that this matter is a product of the active cytoplasm seen in these cells during stages 10–13 and that it is released during the compaction/degradation of these cells during stages 14 and 15. This fits well with previous reports suggesting that the material is tapetum-derived sporopollenin orbicules needed for the formation of the outer walls of spores (Aya *et al.*, 2011; Wallace *et al.*, 2015; Daku *et al.*, 2016).

The behavior of columella and tapetum cells during the later stages of sporangium development was severely compromised in the double mutant. Thus, the compaction and possible loss of cells seen in the WT after stage 11 was completely missing in the double mutant (Figs 3a,b, S6a–c). Also, double mutant cells of both layers directly facing the sporogenous cells completely failed to accumulate active cytoplasm and later failed to deposit extracellular matter, in contrast to their WT counterparts (Fig. 3b). In essence, all signs of the columella and tapetum cell activities accompanying spore formation and maturation in the WT was missing in the double mutant. Together, this clearly shows that endothecium expression of clade II bHLH TFs is not only crucial for maturation of the sporogenous cells, but also for the columella and tapetum cells likely to nurse them.

## Discussion

Clade II bHLH TFs play a conserved role in controlling somatic nursing cells in moss sporangia and angiosperm anthers

Proper development of microsporocytes/microspores/pollen in angiosperm anthers is dependent on nursing functions provided by somatic sporophytic cells, most notably the tapetum. Two main types of tapetum are recognized in plants, the secretory (parietal) type and the amoeboid (periplasmodial) type (Pacini

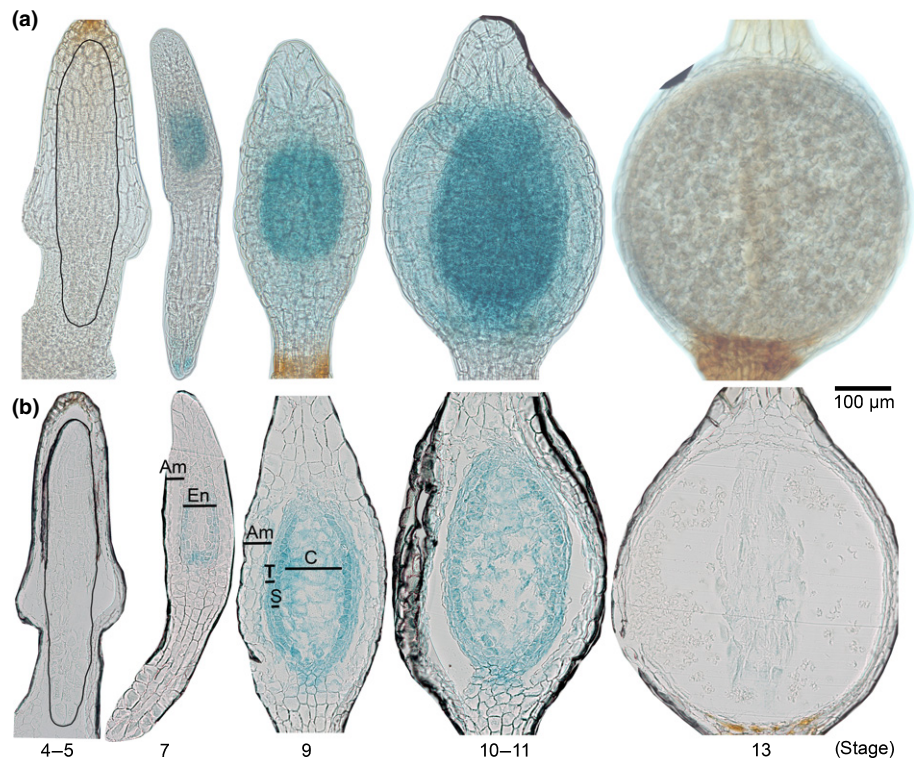






**Fig. 3** Mid- and late-stage development of sporogenous, tapetum and columella cells is deficient in the *Physcomitrium patens* *Ppbhlh092Ppbhlh098* double mutant. (a) Representative longitudinal medial sections through WT and *Ppbhlh092Ppbhlh098-1* sporophytes. Sectioned WT sporophytes range from developmental stage 4 to 15 and dpw-values denote days post watering when these stages peaked in occurrence (see also Table 1). Sectioned double mutant sporophytes were harvested at the same time points as their WT counterparts even if stages equivalent to those in the WT cannot be readily identified from 14 dpw and onwards. Stages 4–7 sporophytes are shown in their entirety while later stage sporophytes have been trimmed to mostly show sporangia. For clarity, gametophytic mother tissues surrounding the sporophytes have been removed from images. For similar series of sporophyte sections showing entire organs with surrounding gametophytic mother tissues for all specimens, and also including the earliest stages, see Supporting Information Fig. S5. Cell layers discussed in the text have been marked in stage 4 and 9 organs for both genotypes: amphithecium (Am); endothecium (En); tapetum (T); sporogenous cells (S); columella (C). Gaps between the Am and En layers frequently seen in stage 9 organs are marked by hash (#) signs. (b) Details at high magnification from representative medial sections through WT sporangia ranging from developmental stage 9 to 15, as well as through *Ppbhlh092Ppbhlh098-1* sporangia harvested at the corresponding time points. Cell types have been marked: tapetum (T); sporogenous cells (S); columella (C); sporocytes (Sc); aberrant/degrading mutant sporocytes (Sc<sup>Δ</sup>); spores (Sp). Asterisks mark active cytoplasm in otherwise vacuolarized cells. Arrows mark deposited extracellular matter. Dpw-values denote days post watering when WT stages peaked in occurrence (see also Table 1). For differential interference contrast images of liberated sporogenous WT cells from stages 11–14, see Fig. S7.

**Fig. 4** *PpbHLH092* translational reporter shows signals in endothecium layers and foot of the *Physcomitrium patens* sporophyte. Whole-mounted (a) and sectioned (b) GUS-stained *PpbHLH092pro::PpbHLH092-GFP* sporophytes ranging from stage 4/5 to 13. Signals were clearly detected in the columella (C), the sporogenous cells (S) and the tapetum (T) layers of the endothecium (En) from stage 7 to stage 10–11, but were essentially missing from the amphithecium (Am). Faint signals were reproducibly detected also in the extreme foot as seen in the stage 7 organ in (a). Numbers below organs indicate probable developmental stages. Stage 4–5 sporophytes lacking signals are still contained within gametophytic mother tissues and they have been traced for clarity.



the sporogenous cells in angiosperm anthers and the sporangium of the model moss *P. patens*. In *P. patens*, these similarities apply to all cells immediately adjacent to the sporogenous cells, that is the innermost tapetum layer and the outermost columella layer, and we propose that these two cell layers have largely similar functions. The three clade II bHLH Arabidopsis genes *AtbHLH010*, *AtbHLH089* and *AtbHLH091* and the *P. patens* homolog *PpbHLH092* are all expressed both in the sporogenous cells and in the tapetal/columella cells surrounding them, with an onset at around when formative cell divisions are completed and a peak at around when the sporogenous cells enter meiosis (Fig. 4; Zhu *et al.*, 2015; Fu *et al.*, 2020). In line with this expression profile, restriction of clade II bHLH TF activity leaves the formative cell divisions unaffected in both species, while maturation/differentiation of the sporogenous cells and the

tapetal/columella cells surrounding them is severely deficient (Figs 3, S6; Zhu *et al.*, 2015). Expansion accompanied by vacuolarization of tapetal/columella cells is initiated in mutants of both species, but these processes completely fail to reverse into compaction/degradation as in the WT. Both moss and Arabidopsis loss-of-function mutants furthermore completely fail to produce functional pollen/spores.

While the three Arabidopsis and two *P. patens* clade II bHLH genes provide largely redundant functions, the two rice homologs *OsTIP2* and *OsEAT1*, being the result of a relatively early monocot-specific gene duplication, have acquired unique and partly sequential functions, as manifested by clear phenotypes when either of the two genes is mutated (this study; Niu *et al.*, 2013; Fu *et al.*, 2014; Ko *et al.*, 2014; Zhu *et al.*, 2015). However, the general pattern from Arabidopsis and *P. patens* can still

be recognized, with expression of both genes in tapetum and sporogenous cells and single loss-of-function mutants showing deficient tapetum compaction/degradation and pollen production (Niu *et al.*, 2013; Fu *et al.*, 2014; Ko *et al.*, 2014). The two rice single mutants also show unique phenotypes. The *Ostip2* mutant exhibits ectopic periclinal divisions of tapetal cells while the *Oseat1* mutant exhibits aberrant extracellular sporopollenin deposition into so-called Ubisch bodies (Niu *et al.*, 2013; Fu *et al.*, 2014; Ko *et al.*, 2014). This fits well with our observations of occasional extra periclinal tapetum cell divisions and a complete lack of sporopollenin orbicule deposition in the *P. patens* *Ppbhlh092Ppbhlh098* double mutant (Fig. 3).

Thus, the findings presented here indicate strongly that moss and angiosperm clade II bHLH TFs provide a functionally conserved role in controlling the sporophytic somatic cells surrounding and nursing the sporogenous cells in sporangia and anthers, respectively. By inference, this lends solid support to the idea that such nursing functions in mosses and angiosperms, lineages separated by *c.* 450 million years of evolution (Morris *et al.*, 2018), are related by descent.

#### Evolutionary origin of clade II bHLH-dependent tapetal-like functions

The fact that clade II bHLH TFs exist in all major land plant lineages (Fig. 1d; Zhang *et al.*, 2020; Zheng *et al.*, 2020) could indicate that tapetal-like functions controlled by this TF family had been established already in the last common ancestor of all extant land plants. This interpretation can be questioned, however, by the notion that tapetal-like functions are difficult to distinguish, or even missing, in liverworts and hornworts, the two lineages which together with mosses make up the bryophytes (Pacini *et al.*, 1985; Wellman, 2004; Wallace *et al.*, 2011; Zheng *et al.*, 2020). Even if they are all unbranched and carry a single terminal sporangium, the difference in tapetum occurrence and appearance is just one of several fundamental differences between the sporophytes of mosses, liverworts and hornworts, possibly indicating considerable diversification of this structure after the evolutionary split of the three lineages (Renzaglia *et al.*, 2000; Shaw *et al.*, 2011; Ligrone *et al.*, 2012). The interrelationship of bryophytes has long been debated, but a monophyletic origin of the three groups with hornworts being the sister of an internal moss and liverwort clade has recently gained increased support (discussed in Frangedakis *et al.*, 2021, and references therein). In light of this, the lack of obvious tapetal tissues in liverworts and hornworts could indicate that elaborate clade II bHLH TF-dependent tapetal functions may have existed in the common ancestors of all extant land plants but were changed beyond easy recognition, or lost, in these two lineages over time. Alternatively, but perhaps less likely, elaborate tapetal functions may have arisen by convergent evolution in mosses and vascular plants from primitive clade II bHLH-dependent precursor functions. In either case, studies of clade II bHLH functions in liverworts and hornworts have the potential to shed light on the origin of tapetal-like functions by providing information about their evolutionary remnants or precursors.

#### Open questions related to the function of tapetal-like nursing cells and their regulation by clade II bHLH TFs in the moss sporangium

Angiosperm clade II bHLH proteins are part of a larger network of TFs which together provide temporal and spatial control of an array of genes needed for proper anther development and pollen production (Gomez *et al.*, 2015; Verma, 2019). Within this network, the functions of clade II and clade III(a+c)1 bHLH TFs appear to be particularly closely intertwined. That genes belonging to one clade are needed for normal transcription of genes belonging to the other, and that BIF-domain-dependent heterodimer formation between gene products of different clades controls nuclear localization and *trans*-activating capacity are recurring general themes evident in both Arabidopsis and rice (Feng *et al.*, 2012; Niu *et al.*, 2013; Fu *et al.*, 2014, 2020; Ko *et al.*, 2014, 2017; Zhu *et al.*, 2015; Cui *et al.*, 2016; Ranjan *et al.*, 2017). The fact that *P. patens* encodes both clade II and clade III(a+c)1 bHLH proteins with seemingly conserved BIF domains that are specifically expressed in developing sporophytes opens the possibility that some of these regulatory interactions were established already in the common ancestors of mosses and angiosperms (Figs 1a,b, S3, S4).

*PpbHLH092* was found to be expressed not only in the sporangium, but also weakly in the foot of developing sporophytes (Fig. 4). However, we could not observe any clear loss-of-function phenotypes in this tissue. While the foot expression could be of limited functional importance, it is also possible that it controls functions not giving obvious morphological consequences when compromised, or that it affects development at a distant site by unknown mechanisms (possibly even the sporangium). Furthermore, both clade II and clade III(a+c)1 bHLH genes also show putative basal expression in some non-sporophytic tissues (Figs 1a,b, S3), and even if we were unable to score obvious phenotypes in gametophytic tissues of the *Ppbhlh092Ppbhlh098* double mutant, it cannot be excluded that genes from one or both clades have functions also in this generation.

In addition to aberrations affecting the tapetum and columella layers, the *Ppbhlh092Ppbhlh098* double mutant also shows an abrupt arrest in the development of sporogenous cells (Fig. 3). Higher resolution methods are needed to pinpoint the exact timing of this arrest in relation to meiotic progression, but our sections at least show that it occurs well before completion of cytokinesis (Fig. 3b). This is in line with rice clade II bHLH loss-of-function mutants which also show arrested/aberrant meiosis (Fu *et al.*, 2014; Ko *et al.*, 2014; Ono *et al.*, 2018), but contrasts with the corresponding Arabidopsis mutants in which meiosis appears normal (Zhu *et al.*, 2015). Premeiotic processes may thus be targets for clade II bHLH regulation in some land plants, but not in others. Another possibility, at least regarding differences between moss and vascular plants, is that they reflect fundamental differences in the sequence of events during meiosis and sporulation. Sporogenesis in bryophytes is known to differ from that in vascular plants, as the initiation of cytokinesis proceeds meiotic nuclear divisions, typically leading to early sporocytes that are



quadrilobed with a centrally positioned diploid nucleus (Brown & Lemmon, 2013). This precocious quadrilobing may represent a relic of the evolutionary process of transferring the sporopollenin coat from the zygote to its meiotic products, as it may have allowed the zygotic nucleus to drive the deposition of wall material around spores in making, before the onset of nuclear divisions (Brown & Lemmon, 2011). Although speculative, this opens the possibility that the target processes of clade II bHLH regulation are the same in both mosses and vascular plants, but that these processes occur at different time points in relation to the completion of meiosis.

At this point, we cannot tell with certainty if the failure of *Ppbbhlb092Ppbbhlb098* sporogenous cells to complete meiosis is caused by the loss of clade II bHLH functions in these cells and/or the loss of such functions in the nursing tapetum and columella cells surrounding them. In angiosperms, an increasing body of evidence suggests that gene expression in the microsporocytes/microspores may be controlled nonautonomously by the tapetal cells (Lei & Liu, 2020, and references therein). Possible mechanisms being discussed include the tapetal production of small RNAs which, directly or indirectly, may control gene expression in the microsporocytes/microspores. Interestingly, the rice clade II bHLH TF *OsEAT1* has been shown to control the biogenesis of small RNAs produced in the tapetum, which hypothetically may control the expression of microsporocyte genes important for meiosis (Ono *et al.*, 2018). Future studies will need to reveal whether this and other putative mechanisms for communication between sporocytes/spores and surrounding diploid somatic nursing tissues may be conserved between angiosperms and mosses.





## Acknowledgements

We thank Ulf Lagercrantz for help with phylogenetic analysis. This work was supported by grants from the Swedish Research Council to ES and MT (621-2014-4941; 2018-04068) and the Nilsson-Ehle Endowments to KL and ML-O (41629).

## Author contributions

ML-O, KL and MT conducted the experimental work and analyzed the data. ML-O, KL, ES and MT designed experiments, interpreted data and wrote the manuscript. ML-O and KL contributed equally to this work.

## ORCID

Katarina Landberg  <https://orcid.org/0000-0002-2945-8571>  
Mauricio Lopez-Obando  <https://orcid.org/0000-0002-1380-0643>  
Eva Sundberg  <https://orcid.org/0000-0003-4228-434X>  
Mattias Thelander  <https://orcid.org/0000-0002-6663-7405>

## Data availability

The data that support the findings of this study are available from the corresponding author upon request.

## References

- Åstrand J, Knight C, Robson J, Talle B, Wilson ZA. 2021. Evolution and diversity of the angiosperm anther: trends in function and development. *Plant Reproduction* 34: 307–319.
- Aya K, Hiwatashi Y, Kojima M, Sakakibara H, Ueguchi-Tanaka M, Hasebe M, Matsuoka M. 2011. The gibberellin perception system evolved to regulate a pre-existing GAMYB-mediated system during land plant evolution. *Nature Communications* 2: 544.
- Berger F, Twell D. 2011. Germline specification and function in plants. *Annual Review of Plant Biology* 62: 461–484.
- Brown RC, Lemmon BE. 2011. Spores before sporophytes: hypothesizing the origin of sporogenesis at the algal–plant transition. *New Phytologist* 190: 875–881.
- Brown RC, Lemmon BE. 2013. Sporogenesis in Bryophytes: patterns and diversity in meiosis. *Botanical Review* 79: 178–280.
- Catarino B, Hetherington AJ, Emms DM, Kelly S, Dolan L. 2016. The stepwise increase in the number of transcription factor families in the precambrian predated the diversification of plants on land. *Molecular Biology and Evolution* 33: 2815–2819.
- Chang J-M, Di Tommaso P, Notredame C. 2014. TCS: a new multiple sequence alignment reliability measure to estimate alignment accuracy and improve phylogenetic tree reconstruction. *Molecular Biology and Evolution* 31: 1625–1637.
- Colpitts CC, Kim SS, Posehn SE, Jepson C, Kim SY, Wiedemann G, Reski R, Wee AGH, Douglas CJ, Suh D-Y. 2011. PpASCL, a moss ortholog of anther-specific chalcone synthase-like enzymes, is a hydroxyalkylpyrone synthase involved in an evolutionarily conserved sporopollenin biosynthesis pathway. *New Phytologist* 192: 855–868.
- Coudert Y, Novak O, Harrison CJ. 2019. A KNOX-cytokinin regulatory module predates the origin of indeterminate vascular plants. *Current Biology* 29: 2743–2750.
- Cui J, You C, Zhu E, Huang Q, Ma H, Chang F. 2016. Feedback regulation of DYT1 by interactions with downstream bHLH factors promotes DYT1 nuclear localization and anther development. *Plant Cell* 28: 1078–1093.
- Daku RM, Rabbi F, Buttigieg J, Coulson IM, Horne D, Martens G, Ashton MW, Suh D-Y. 2016. PpASCL, the *Physcomitrella patens* anther-specific chalcone synthase-like enzyme implicated in sporopollenin biosynthesis, is needed for integrity of the moss spore wall and spore viability. *PLoS ONE* 11: e0146817.
- Feng B, Lu D, Ma X, Peng Y, Sun Y, Ning G, Ma H. 2012. Regulation of the *Arabidopsis* anther transcriptome by DYT1 for pollen development. *The Plant Journal* 72: 612–624.
- Fernandez-Pozo N, Haas FB, Meyberg R, Ullrich KK, Hiss M, Perroud PF, Hanke S, Kratz V, Powell AF, Vesty EF *et al.* 2020. PEATmoss (*Physcomitrella* expression atlas tool): a unified gene expression atlas for the model plant *Physcomitrella patens*. *The Plant Journal* 102: 165–177.
- Frangedakis E, Shimamura M, Villarreal JC, Li F-W, Tomaselli M, Waller M, Sakakibara K, Renzaglia KS, Szövényi P. 2021. The hornworts: morphology, evolution and development. *New Phytologist* 229: 735–754.
- Fu Y, Li M, Zhang S, Yang Q, Zhu E, You C, Qia J, Ma H, Chang F. 2020. Analyses of functional conservation and divergence reveal requirement of bHLH010/089/091 for pollen development at elevated temperature in *Arabidopsis*. *Journal of Genetics and Genomics* 47: 477–492.
- Fu Z, Yu J, Cheng X, Zong X, Xu J, Chen M, Li Z, Zhang D, Lianga W. 2014. The rice basic helix-loop-helix transcription factor TDR INTERACTING PROTEIN2 is a central switch in early anther development. *Plant Cell* 26: 1512–1524.
- Goldberg RB, Beals TP, Sanders PM. 1993. Anther development: basic principles and practical applications. *Plant Cell* 5: 1217–1229.
- Gomez JF, Talle B, Wilson ZA. 2015. Anther and pollen development: a conserved developmental pathway. *Journal of Integrative Plant Biology* 57: 876–891.
- Graham LE, Cook ME, Busse JS. 2000. The origin of plants: body plan changes contributing to a major evolutionary radiation. *Proceedings of the National Academy of Sciences, USA* 97: 4535–4540.

- Hackenberg D, Twell D. 2019. The evolution and patterning of male gametophyte development. *Current Topics in Developmental Biology* 131: 257–298.
- Haeussler M, Schönig K, Eckert H, Eschstruth A, Mianné J, Renaud J-B, Schneider-Maunoury S, Shkumatava A, Teboul L, Kent J *et al.* 2016. Evaluation of off-target and on-target scoring algorithms and integration into the guide RNA selection tool CRISPOR. *Genome Biology* 17: 148.
- Harrison CJ. 2017. Development and genetics in the evolution of land plant body plans. *Philosophical Transactions of the Royal Society B: Biological Sciences* 372: 20150490.
- Hiss M, Meyberg R, Westermann J, Haas FB, Schneider L, Schallenberg-Rudinger M, Ullrich KK, Rensing SA. 2017. Sexual reproduction, sporophyte development and molecular variation in the model moss *Physcomitrella patens*: introducing the ecotype Reute. *The Plant Journal* 90: 606–620.
- Jung K-H, Han M-J, Lee Y-S, Kim Y-W, Hwang I, Kim M-J, Kim Y-K, Nahm BH, An G. 2005. Rice undeveloped Tapetum1 is a major regulator of early tapetum development. *Plant Cell* 17: 2705–2722.
- Ko S-S, Li M-J, Ku MS-B, Ho Y-C, Lin Y-J, Chuang M-H, Hsing H-X, Lien Y-C, Yang H-T, Chang H-C *et al.* 2014. The bHLH142 transcription factor coordinates with TDR1 to modulate the expression of *EAT1* and regulate pollen development in rice. *Plant Cell* 26: 2486–2504.
- Ko S-S, Li M-J, Lin Y-J, Hsing H-X, Yang T-T, Chen T-K, Zhong C-M, Ku MS-B. 2017. Tightly controlled expression of *bHLH142* is essential for timely tapetal programmed cell death and pollen development in rice. *Frontiers in Plant Science* 8: 1258.
- Kofuji R, Yoshimura T, Inoue H, Sakakibara K, Hiwatashi Y, Kurata T, Aoyama T, Ueda K, Hasebe M. 2009. Gametangia development in the moss *Physcomitrella patens*. *Annual Plant Reviews* 36: 167–181.
- Kumar S, Stecher G, Li M, Knyaz C, Tamura K. 2018. MEGA X: molecular evolutionary genetics analysis across computing platforms. *Molecular Biology and Evolution* 35: 1547–1549.
- Landberg K, Simura J, Ljung K, Sundberg E, Thelander M. 2020. Studies of moss reproductive development indicate that auxin biosynthesis in apical stem cells may constitute an ancestral function for focal growth control. *New Phytologist* 229: 845–860.
- Lei X, Liu B. 2020. Tapetum-dependent male meiosis progression in plants: increasing evidence emerges. *Frontiers in Plant Science* 10: 1667.
- Li N, Zhang DS, Liu HS, Yin CS, Li XX, Liang WQ, Yuan Z, Xu B, Chu HW, Wang J *et al.* 2006. The rice Tapetum degeneration Retardation gene is required for tapetum degradation and anther development. *Plant Cell* 18: 2999–3014.
- Ligrone R, Duckett JG, Renzaglia KS. 2012. Major transitions in the evolution of early land plants: a bryological perspective. *Annals of Botany* 109: 851–871.
- Lopez-Obando M, Hoffmann B, Géry C, Guyon-Debast A, Téoulé E, Rameau C, Bonhomme S, Nogué F. 2016. Simple and efficient targeting of multiple genes through CRISPR-Cas9 in *Physcomitrella patens*. *G3 (Bethesda)* 6: 3647–3653.
- Ma X, Wu Y, Zhang G. 2021. Formation pattern and regulatory mechanisms of pollen wall in *Arabidopsis*. *Journal of Plant Physiology* 260: 153388.
- Mallett DR, Chang M, Cheng X, Bezanilla M. 2019. Efficient and modular CRISPR-Cas9 vector system for *Physcomitrella patens*. *Plant Direct* 3: e00168.
- Modrzejewski D, Hartung F, Lehnert H, Sprink T, Kohl C, Keilwagen J, Wilhelm R. 2020. Which factors affect the occurrence of off-target effects caused by the use of CRISPR/Cas: a systematic review in plants. *Frontiers in Plant Science* 11. doi: 10.3389/fpls.2020.574959.
- Morris JL, Puttick MN, Clark JW, Edwards D, Kenrick P, Pressel S, Wellman CH, Yang Z, Schneider H, Donoghue PCJ. 2018. The timescale of early land plant evolution. *Proceedings of the National Academy of Sciences, USA* 115: E2274–E2283.
- Niu N, Liang W, Yang X, Jin W, Wilson ZA, Hu J, Zhang D. 2013. *EAT1* promotes tapetal cell death by regulating aspartic proteases during male reproductive development in rice. *Nature Communications* 4: 1445.
- Notredame C, Higgins DG, Heringa J. 2000. T-Coffee: a novel method for fast and accurate multiple sequence alignment. *Journal of Molecular Biology* 302: 205–217.
- Ono S, Liu H, Tsuda K, Fukai E, Tanaka K, Sasaki T, Nonomura K-I. 2018. *EAT1* transcription factor, a non-cell-autonomous regulator of pollen production, activates meiotic small RNA biogenesis in rice anther tapetum. *PLoS Genetics* 14: e1007238.
- Ortiz-Ramirez C, Hernandez-Coronado M, Thamm A, Catarino B, Wang M, Dolan L, Feijo JA, Becker JD. 2016. A transcriptome atlas of *Physcomitrella patens* provides insights into the evolution and development of land plants. *Molecular Plant* 9: 205–220.
- Pacini E, Franchi GG, Hesse M. 1985. The tapetum: its form, function, and possible phylogeny in Embryophyta. *Plant Systematics and Evolution* 149: 155–185.
- Parish RW, Li SF. 2010. Death of a tapetum: a programme of developmental altruism. *Plant Science* 178: 73–89.
- Perroud PF, Haas FB, Hiss M, Ullrich KK, Alboresi A, Amirebrahimi M, Barry K, Bassi R, Bonhomme S, Chen H *et al.* 2018. The *Physcomitrella patens* gene atlas project: large-scale RNA-seq based expression data. *The Plant Journal* 95: 168–182.
- Pires N, Dolan L. 2010. Origin and diversification of basic-helix-loop-helix proteins in plants. *Molecular Biology and Evolution* 27: 862–874.
- Ranjan R, Khurana R, Malik N, Badoni S, Parida SK, Kapoor S, Tyagi AK. 2017. bHLH142 regulates various metabolic pathway-related genes to affect pollen development and anther dehiscence in rice. *Scientific Reports* 7: 43397.
- Regmi KC, Gaxiola RA. 2017. Alternate modes of photosynthate transport in the alternating generations of *Physcomitrella patens*. *Frontiers in Plant Science* 8: 1956.
- Renzaglia KS, Duff RJ, Nickrent DL, Garbary DJ. 2000. Vegetative and reproductive innovations of early land plants: implications for a unified phylogeny. *Philosophical Transactions of the Royal Society of London. Series B: Biological Sciences* 355: 769–793.
- Sakakibara K, Nishiyama T, Deguchi H, Hasebe M. 2008. Class 1 KNOX genes are not involved in shoot development in the moss *Physcomitrella patens* but do function in sporophyte development. *Evolution and Development* 10: 555–566.
- Sanders PM, Bui AQ, Weterings K, McIntire KN, Hsu Y-C, Lee PY, Truong MT, Beals TP, Goldberg RB. 1999. Anther developmental defects in *Arabidopsis thaliana* male-sterile mutants. *Sexual Plant Reproduction* 11: 297–322.
- Schaefer D, Zryd J-P, Knight CD, Cove DJ. 1991. Stable transformation of the moss *Physcomitrella patens*. *Molecular and General Genetics* 226: 418–424.
- Schindelin J, Arganda-Carreras I, Frise E, Kaynig V, Longair M, Pietzsch T, Preibisch S, Rueden C, Saalfeld S, Schmid B *et al.* 2012. Fiji: an open-source platform for biological-image analysis. *Nature Methods* 9: 676–682.
- Shaw AJ, Szövényi P, Shaw B. 2011. Bryophyte diversity and evolution: windows into the early evolution of land plants. *American Journal of Botany* 98: 352–369.
- Sorensen A-M, Kröber S, Unte US, Huijser P, Dekker K, Saedler H. 2003. The *Arabidopsis* *ABORTED MICROSPORES (AMS)* gene encodes a MYC class transcription factor. *The Plant Journal* 33: 413–423.
- Thelander M, Landberg K, Sundberg E. 2019. Minimal auxin sensing levels in vegetative moss stem cells revealed by a ratiometric reporter. *New Phytologist* 224: 775–788.
- Thelander M, Nilsson A, Olsson T, Johansson M, Girod PA, Schaefer DG, Zryd JP, Ronne H. 2007. The moss genes *PpSK11* and *PpSK12* encode nuclear SnRK1 interacting proteins with homologues in vascular plants. *Plant Molecular Biology* 64: 559–573.
- Verma N. 2019. Transcriptional regulation of anther development in *Arabidopsis*. *Gene* 689: 202–209.
- Wallace IM, O'Sullivan O, Higgins DG, Notredame C. 2006. M-Coffee: combining multiple sequence alignment methods with T-Coffee. *Nucleic Acids Research* 34: 1692–1699.
- Wallace S, Chater CC, Kamisugi Y, Cuming AC, Wellman CH, Beerling DJ, Fleming AJ. 2015. Conservation of *Male Sterility 2* function during spore and pollen wall development supports an evolutionarily early recruitment of a core

- component in the sporopollenin biosynthetic pathway. *New Phytologist* 205: 390–401.
- Wallace S, Fleming A, Wellman CH, Beerling DJ. 2011. Evolutionary development of the plant spore and pollen wall. *AoB Plants* 2011. doi: 10.1093/aobpla/plr027.
- Wellman CH. 2004. Origin, function and development of the spore wall in early land plants. In: Hemsley AR, Poole I, eds. *Evolution of plant physiology*. London, UK: Elsevier & Academic Press, 43–63.
- Xu J, Yang C, Yuan Z, Zhang D, Gondwe MY, Ding Z, Liang W, Zhang D, Wilson ZA. 2010. The *ABORTED MICROSPORES* regulatory network is required for postmeiotic male reproductive development in *Arabidopsis thaliana*. *Plant Cell* 22: 91–107.
- Yip HK, Floyd SK, Sakakibara K, Bowman JL. 2016. Class III HD-Zip activity coordinates leaf development in *Physcomitrella patens*. *Developmental Biology* 419: 184–197.
- Zhang J, Fu XX, Li RQ, Zhao X, Liu Y, Li MH, Zwaenepoel A, Ma H, Goffinet B, Guan YL *et al.* 2020. The hornwort genome and early land plant evolution. *Nature Plants* 6: 107–118.
- Zhang W, Sun Y, Timofejeva L, Chen C, Grossniklaus U, Ma H. 2006. Regulation of *Arabidopsis tapetum* development and function by *DYSFUNCTIONAL TAPETUM1 (DYT1)* encoding a putative bHLH transcription factor. *Development* 133: 3085–3095.
- Zheng X, He L, Liu Y, Mao Y, Wang C, Zhao B, Li Y, He H, Guo S, Zhang L *et al.* 2020. A study of male fertility control in *Medicago truncatula* uncovers an evolutionarily conserved recruitment of two tapetal bHLH subfamilies in plant sexual reproduction. *New Phytologist* 228: 1115–1133.
- Zhu E, You C, Wang S, Cui J, Niu B, Wang Y, Qi J, Ma H, Chang F. 2015. The DYT1-interacting proteins bHLH010, bHLH089 and bHLH091 are redundantly required for *Arabidopsis* anther development and transcriptome. *The Plant Journal* 83: 976–990.

## Supporting Information

Additional Supporting Information may be found online in the Supporting Information section at the end of the article.

**Fig. S1** Schematic overviews showing how loss-of-function mutants and translational reporter lines were generated.

**Fig. S2** Amino acid sequence alignment used to infer phylogenetic tree shown in Fig. 1(d).

**Fig. S3** Relative expression of clade II and clade III(a+c)1 *Physcomitrella patens* bHLH TFs in various tissues, as indicated by publicly available expression data.

**Fig. S4** Amino acid sequence alignment of clade II bHLH TFs from representative land plant species.

**Fig. S5** Representative longitudinal medial sections through sporophytes of different developmental stages from the WT and the *Ppbhlh092Ppbhlh098-1* double mutant.

**Fig. S6** Early columella expansion, late columella and tapetum compaction, and late loss of discernable columella cells are all compromised in the *Ppbhlh092Ppbhlh098* double mutant.

**Fig. S7** Appearance of liberated WT sporogenous cells from stages 11 to 14 of development.

**Table S1** Characteristics of crRNA (crRNAs) in gRNA-expressing plasmids.

**Table S2** Primers used in study.

**Table S3** Characteristics of knock-out and knock-in lines obtained by CRISPR-CAS9 gene editing.

Please note: Wiley Blackwell are not responsible for the content or functionality of any Supporting Information supplied by the authors. Any queries (other than missing material) should be directed to the *New Phytologist* Central Office.

See also the Commentary on this article by Levins *et al.*, 235: 377–379.